



# Pandoravirus Celtis Illustrates the Microevolution Processes at Work in the Giant *Pandoraviridae* Genomes

Matthieu Legendre<sup>1</sup>, Jean-Marie Alempic<sup>1</sup>, Nadège Philippe<sup>1</sup>, Audrey Lartigue<sup>1</sup>, Sandra Jeudy<sup>1</sup>, Olivier Poirot<sup>1</sup>, Ngan Thi Ta<sup>1</sup>, Sébastien Nin<sup>1</sup>, Yohann Couté<sup>2</sup>, Chantal Abergel<sup>1\*</sup> and Jean-Michel Claverie<sup>1\*</sup>

<sup>1</sup> Aix Marseille Univ, CNRS, IGS, Structural and Genomic Information Laboratory (UMR7256), Mediterranean Institute of Microbiology (FR3479), Marseille, France, <sup>2</sup> Inserm, BIG-BGE, CEA, Université Grenoble Alpes, Grenoble, France

## OPEN ACCESS

### Edited by:

Ricardo Flores,  
Instituto de Biología Molecular y  
Celular de Plantas (IBMCP), Spain

### Reviewed by:

Amparo Latorre,  
University of Valencia, Spain  
Victor Krylov,  
I. I. Mechnikov Research Institute  
for Vaccines and Sera (RAS), Russia

### \*Correspondence:

Chantal Abergel  
chantal.abergel@igs.cnrs-mrs.fr  
Jean-Michel Claverie  
jean-michel.claverie@univ-amu.fr

### Specialty section:

This article was submitted to  
Virology,  
a section of the journal  
Frontiers in Microbiology

**Received:** 18 December 2018

**Accepted:** 19 February 2019

**Published:** 08 March 2019

### Citation:

Legendre M, Alempic J-M,  
Philippe N, Lartigue A, Jeudy S,  
Poirot O, Ta NT, Nin S, Couté Y,  
Abergel C and Claverie J-M (2019)  
Pandoravirus Celtis Illustrates  
the Microevolution Processes at Work  
in the Giant Pandoraviridae Genomes.  
Front. Microbiol. 10:430.  
doi: 10.3389/fmicb.2019.00430

With genomes of up to 2.7 Mb propagated in  $\mu\text{m}$ -long oblong particles and initially predicted to encode more than 2000 proteins, members of the *Pandoraviridae* family display the most extreme features of the known viral world. The mere existence of such giant viruses raises fundamental questions about their origin and the processes governing their evolution. A previous analysis of six newly available isolates, independently confirmed by a study including three others, established that the *Pandoraviridae* pan-genome is open, meaning that each new strain exhibits protein-coding genes not previously identified in other family members. With an average increment of about 60 proteins, the gene repertoire shows no sign of reaching a limit and remains largely coding for proteins without recognizable homologs in other viruses or cells (ORFans). To explain these results, we proposed that most new protein-coding genes were created *de novo*, from pre-existing non-coding regions of the G+C rich pandoravirus genomes. The comparison of the gene content of a new isolate, pandoravirus celtis, closely related (96% identical genome) to the previously described p. quercus is now used to test this hypothesis by studying genomic changes in a microevolution range. Our results confirm that the differences between these two similar gene contents mostly consist of protein-coding genes without known homologs, with statistical signatures close to that of intergenic regions. These newborn proteins are under slight negative selection, perhaps to maintain stable folds and prevent protein aggregation pending the eventual emergence of fitness-increasing functions. Our study also unraveled several insertion events mediated by a transposase of the hAT family, 3 copies of which are found in p. celtis and are presumably active. Members of the *Pandoraviridae* are presently the first viruses known to encode this type of transposase.

**Keywords:** *de novo* gene creation, comparative genomics, *Acanthamoeba*, giant viruses, soil viruses, hAT transposase

## INTRODUCTION

The *Pandoraviridae* is a proposed family of giant dsDNA viruses - not yet registered by the International Committee on Taxonomy of Viruses (ICTV) - multiplying in various species of *Acanthamoeba* through a lytic infectious cycle. Their linear genomes, flanked by large terminal repeats, range from 1.9 to 2.7 Mb in size, and are propagated in elongated oblong particles approximately 1.2  $\mu\text{m}$  long and 0.6  $\mu\text{m}$  in diameter (**Supplementary Figure S1**). The prototype

strain (and the one with the largest known genome) is pandoravirus salinus (*p. salinus*), isolated from shallow marine sediments off the coast of central Chile (Philippe et al., 2013). Other members were soon after isolated from worldwide locations. Complete genome sequences have been determined for *p. dulcis* (Melbourne, Australia) (Philippe et al., 2013), *p. inopinatum* (Germany) (Antwerpen et al., 2015), *p. macleodensis* (Melbourne, Australia), *p. neocaledonia* (New Caledonia), and *p. quercus* (France) (Legendre et al., 2018), and three isolates from Brazil (*p. braziliensis*, *p. pampulha*, and *p. massiliensis*) (Aherfi et al., 2018). A standard phylogenetic analysis of the above strains suggested that the *Pandoraviridae* family consists of two separate clades (Claverie et al., 2018; **Figure 1**). The average proportion of identical amino acids between pandoravirus orthologs within each clade is above 70% while it is below 55% between members of the A and B clades. Following a stringent reannotation of the predicted protein-coding genes using transcriptomic and proteomic data, our comparative genomic analysis reached the main following conclusions (Legendre et al., 2018):

- (1) The uniquely large proportion of predicted proteins without homologs outside of the *Pandoraviridae* (ORFans) is real and not due to bioinformatic errors induced by the above-average G+C content (>60%) of pandoravirus genomes;
- (2) the *Pandoraviridae* pan genome appears “open” (i.e., unbounded);
- (3) as most of the genes are unique to each strain are ORFans, they were not horizontally acquired from other (known) organisms;
- (4) they are neither predominantly the result of gene duplications.

The scenario of *de novo* and *in situ* gene creation, supported by the analysis of their sequence statistical signatures, thus became our preferred explanation for the origin of strain specific genes.

In the present study, we take advantage of the high similarity (96.7% DNA sequence identity) between *p. quercus* and a newly characterized isolate, *p. celtis*, to investigate the microevolution processes initiating the divergence between pandoraviruses. Our results further support *de novo* gene creation as a main diversifying force of the *Pandoraviridae* family.

## MATERIALS AND METHODS

### Virus Isolation, Production, and Purification

*P. celtis* and *p. quercus* were isolated in November 2014 from samples of surface soil taken at the base of two trees (*Celtis australis* and *Quercus ilex*) less than 50 m apart in an urban green space of Marseille city (GPS: 43°15'16.00"N, 5°25'4.00"E). Their particles were morphologically identical to previously characterized pandoraviruses (**Supplementary Figure S1**). The viral populations were amplified by co-cultivation with *Acanthamoeba castellanii*. They were then

cloned, mass-produced and purified as previously described (Philippe et al., 2013).

### Genome and Transcriptome Sequencing, Annotation

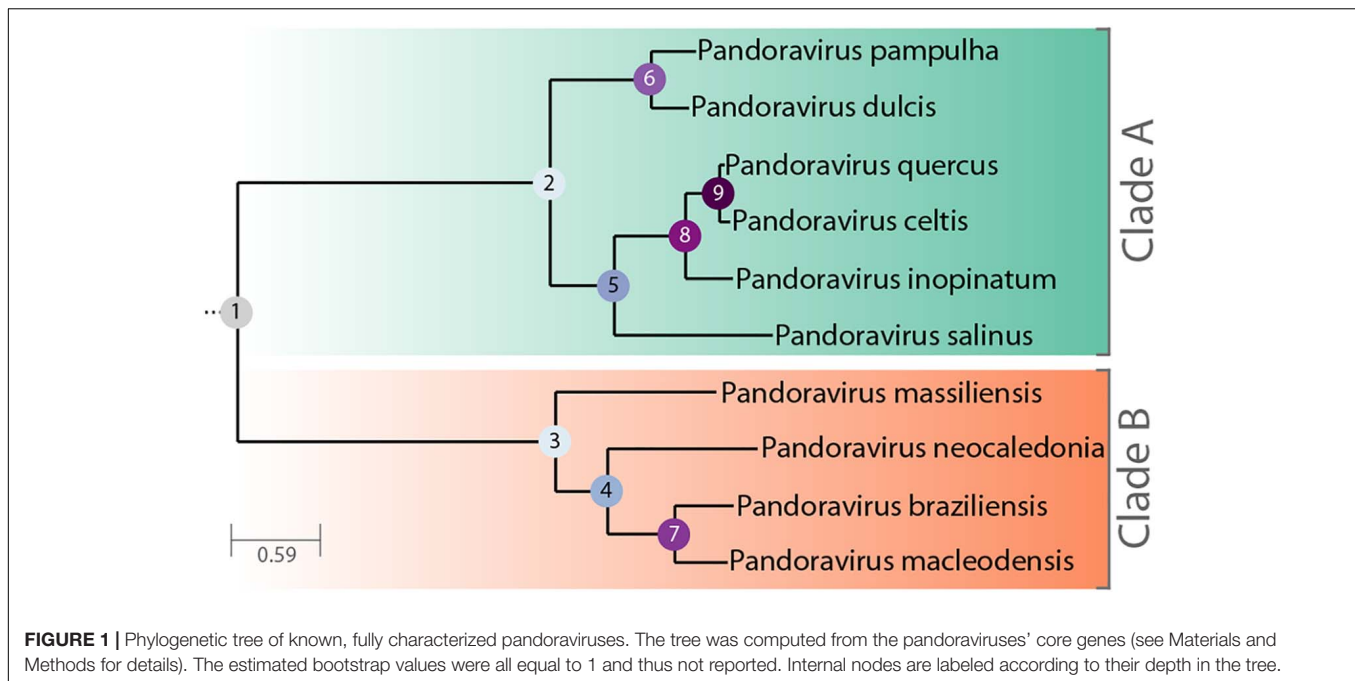
The *p. celtis* genome was fully assembled from one PacBio SMRT cell sequence data with the HGAP 4 assembler (Chin et al., 2013) from the SMRT link package version 5.0.1.9585 with default parameters and the “aggressive” option = true. Genome polishing was finally performed using the SMRT package. Stringent gene annotation was performed as previously described (Legendre et al., 2018). Briefly, data from proteomic characterization of the purified virions were combined with stranded RNA-seq transcriptomic data, as well as protein homology among previously characterized pandoraviruses. The transcriptomic data were generated from cells collected every hour over an infectious cycle of 15 h. They were pooled and RNAs were extracted prior poly(A)<sup>+</sup> enrichment. The RNA were then sent for sequencing. Stranded RNA-seq reads were then used to accurately annotate protein-coding as well as non-coding RNA genes. A threshold of gene expression (median read coverage > 5 over the whole transcript) larger than the lowest one associated to proteins detected in proteomic analyses was required to validate all predicted genes (including novel genes) (**Table 1**). Genomic regions exhibiting similar expression levels but did not encompass predicted proteins or did overlap with protein-coding genes expressed from opposite strands were annotated as “non-coding RNA” (ncRNA) after assembly by Trinity (Grabherr et al., 2011). When only genomic data were available, namely for *p. pampulha*, *p. massiliensis*, and *p. braziliensis* (Aherfi et al., 2018), we annotated protein-coding genes using *ab initio* prediction coupled with sequence conservation information as previously described (Legendre et al., 2018).

Gene clustering was performed on all available pandoraviruses' protein sequences using Orthofinder (Emms and Kelly, 2015) with defaults parameters except for the “msa” option for the gene tree inference method.

Functional annotation of protein-coding genes was performed using a combination of protein domains search with the CD-search tool (Marchler-Bauer and Bryant, 2004) and HMM-HMM search against the Uniclust30 database with the HHblits tool (Remmert et al., 2011). In addition, we used the same procedure to update the functional gene annotation of *p. salinus*, *p. dulcis*, *p. quercus*, *p. macleodensis*, and *p. neocaledonia* (Genbank IDs: KC977571, KC977570, MG011689, MG011691, and MG011690).

### Phylogenetic and Selection Pressure Analysis

The phylogenetic tree (**Figure 1**) was computed from the concatenated multiple alignment of the sequences of pandoraviruses' core proteins corresponding to single-copy genes. The alignments of orthologous genes peptide sequences were done using Mafft (Katoh et al., 2002). The tree was computed using IQtree (Hoang et al., 2018) with the following options: -m MFP -bb 10000 -st codon -bnni. The best model chosen was: GY+F+R5. Codon sequences were subsequently



mapped on these alignments. Ratios of non-synonymous (dN) over synonymous (dS) mutation rates for pairs of orthologous genes were computed using the YN00 method from the PAML package (Yang, 2007). Filters were applied so that dN/dS ratios were only considered if: dN > 0, dS > 0, dS ≤ 2 and dN/dS ≤ 10. We also computed the Codon Adaptation Index (CAI) of *p. celtis* genes using the cai tool from the Emboss package (Rice et al., 2000) as previously described (Legendre et al., 2018).

## Particle Proteomics

The *p. celtis* particle proteome was characterized by mass spectrometry-based proteomics from purified viral particles as previously described (Legendre et al., 2015, 2018).

## RESULTS

### Main Structural Features of the *P. celtis* and *P. quercus* Genomes

The *p. celtis* dsDNA genome sequence was assembled as a single 2,028,440 bp-long linear contig, thus slightly shorter than the published 2,077,288-bp for *p. quercus*. Both contains 61% of G+C. The two genomes exhibit a global collinearity well illustrated by a dotplot comparison of their highly similar nucleotide sequences (Figure 2). In particular, their 48.8 kb difference in genome size does not obviously correspond to a large non-homologous region or a large-scale duplication. Both genomes begin by a nearly perfect 19-kb long palindrome (labeled “P” in Figure 2). As we did not observe this feature in the other published pandoravirus sequences, it may be specific of *p. celtis* and *p. quercus*, or its absence in other genomes may result from flaws in the assembly of terminal sequences due to insufficient read coverage or quality. Six kb downstream, *p. quercus* exhibits

a segment ([25,480–43,420]) nearly identical (20 indels) to the distal end of the genome, inverted (labeled “T” in Figure 2). Remnants of a similar feature appear blurred in *p. celtis*, but are absent from the other pandoravirus genomes. As these regions are accurately determined, we can infer that a duplication followed by an inversion/translocation of the distal genome terminus occurred in the ancestor of *p. quercus* and *p. celtis* (between node 8 and 9 in Figure 1).

The next noticeable structural rearrangements consist of three segments denoted  $S_0$ ,  $S_1$ , and  $S_2$  in Figure 2. Each of these segments are flanked by terminal inverted repeats (Supplementary Figure S2) and encode a protein (respectively *pclt\_cds\_98*, *pclt\_cds\_672*, and *pclt\_cds\_871*) exhibiting both a BED zinc finger domain and a C-terminal dimerisation region, typical of transposases of the hobo/Activator/Tam3 (hAT) family. All these proteins exhibit the intact signature of hAT transposases and are thus probably active (Atkinson, 2015). Using these sequences as queries, we readily identified other well-conserved hAT transposase homologs in *p. pampulha* (*ppam\_cds\_67*, *cds\_531*, *cds\_663*), *p. macleodensis* (*pmac\_cds\_424*, *cds\_799*, *cds\_869*) and *p. neocaledonia* (*pneo\_cds\_387*, *cds\_113*, *cds\_658*, *cds\_798*).

Besides their common transposase, the  $S_0$  [10.3 kb, pos. 152,985–163,291],  $S_1$  [10.3 kb, pos. 1,156,443–1,166,965], and  $S_2$  [7.3 kb, pos. 1,452,773–1,460,053] transposons encode different sets of proteins.  $S_0$  encodes 9 proteins (*pclt\_cds\_90-98*). Except for the transposase, all of them have no predicted function, and no recognizable homologs outside of the *Pandoraviridae* (i.e., they are “family ORFans”).  $S_1$  encodes 11 proteins (*pclt\_cds\_672-682*) all of which also have no functional attributes and are family ORFans, except for the transposase.  $S_2$  encodes 7 proteins (*pclt\_cds\_865-871*), all of which have no recognizable signature (except for the transposase and a F-box domain for

**TABLE 1** | *P. celtis* and *p. quercus* unique protein-coding genes.

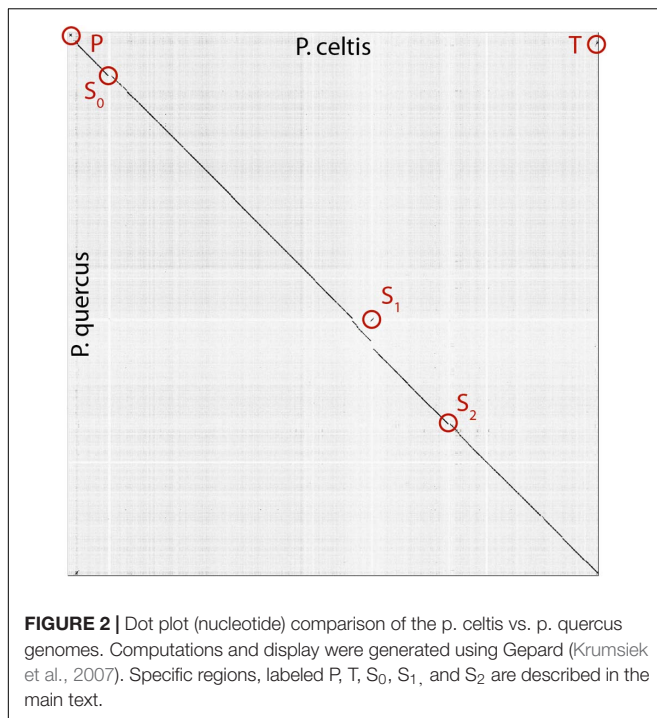
Gene #	Size (aa)	Most ancestral detection	Homolog in <i>p. quercus</i>	Predicted DNA binding	Median RNAseq read coverage
pclt_cds_11	69	Since node 5	None	Yes	704
pclt_cds_308	181	Since node 2	pqer_ncRNA_47	No	986
pclt_cds_350	121	Since node 9	Intergenic	Yes	57
pclt_cds_376	145	Since node 5	3'UTR pqer_cds_371	Yes	454
pclt_cds_725	104	None	None	Yes	46
pclt_cds_870	205	Since node 2	None	Yes	2027
pclt_cds_995	149	Since node 5	5'UTR pqer_cds_981	Yes	13
pclt_cds_1081	125	Since node 8	5'UTR pqer_cds_1061	Yes	12,090
pclt_cds_1084	114	Since node 8	intergenic	Yes	130
<b>Homolog in <i>p. celtis</i></b>					
pqer_cds_6	76	Since node 8	None	Yes	311
pqer_cds_13	117	Since node 5	Intergenic	Yes	99
pqer_cds_17	82	Since node 2	Intergenic	Yes	482
pqer_cds_53	85	Since node 8	Intergenic	Yes	48
pqer_cds_143	93	Since node 8	Anti 5'UTR pclt_cds_146	Yes	177
pqer_cds_151	71	Since node 9	Intergenic	Yes	21
pqer_cds_203	101	Since node 8	Antisense pclt_cds_206	Yes	528
pqer_cds_350	94	None	None	No	160
pqer_cds_474	74	Since node 9	Intergenic	Yes	114
pqer_cds_486	146	Since node 2	3'UTR pclt_cds_499	Yes	71
pqer_cds_665	114	None	None	Yes	1,955
pqer_cds_673	383	None	None	Yes	656
pqer_cds_685	124	Since node 8	Alternative frame pclt_cds_685	No	117
pqer_cds_736	121	Since node 9	Intergenic	Yes	70
pqer_cds_875	136	None	None	No	2,050
pqer_cds_876	74	Since node 2	None	No	1,695
pqer_cds_877	78	None	None	Yes	320
pqer_cds_878	224	None	None	Yes	231
pqer_cds_1061	152	Since node 8	Alternative frame pclt_cds_1081	Yes	14,186
pqer_cds_1178	84	Since node 9	Anti 5'UTR pclt_cds_1203	Yes	170
pqer_cds_1183	158	Since node 2	None	Yes	198

pclt\_cds\_870). Besides the transposase, a single protein have paralogs in the  $S_0$ ,  $S_1$ , and  $S_2$  transposons (pclt\_cds\_92, 681, 869), and one is only shared by  $S_0$  and  $S_1$  (pclt\_cds\_94, 678). These differences clearly suggest that  $S_0$ ,  $S_1$ ,  $S_2$  are not the results of recent duplication/transposition events from a common template.

A tentative scenario for the insertion of the *p. celtis* hAT transposons was inferred from their presence/absence in *p. quercus* and the sequence similarity of the transposases. The  $S_1$  transposon is the only one shared between the two strains (**Supplementary Figure S2**). Moreover, all the orthologous proteins encoded in  $S_1$  are 100% identical (pclt\_cds\_672-682 vs. pqer\_cds\_619-610), including the transposases (pclt\_cds\_672 and pqer\_cds\_619). A first possibility is that the  $S_1$  segment was already present in the ancestor of *p. celtis* and *p. quercus* (**Figure 1**, node 9), then was inverted and translocated about 70 kb downstream from its initial location in *p. celtis*. However, since this transposon is absent from *p. inopinatum* (diverging after node 8, **Figure 1**), it may have been independently gained from the same source into *p. celtis* and *p. quercus* just after

their divergence as two variants within the local viral population. Interestingly, an unrelated sequence of 30.5 kb was inserted at the homologous positions in *p. quercus* (pos. 1,177,379–1,207,935) (**Supplementary Figure S2**). This insertion encodes 24 proteins (pqer\_cds\_659-682) 13 of which are anonymous and ORFans (i.e., only homologous to other pandoraviruses' proteins), the other exhibiting uninformative motifs such as ankyrin repeats (pqer\_cds\_668, 669, 674-676, 680), F-box domains (pqer\_cds\_681, 682), Morn repeat (pqer\_cds\_661) and Ring domain (pqer\_cds\_670). One protein (pqer\_cds\_673) exhibits a low ( $E < 10^{-2}$ ) and partial similarity with a domain found at the N terminus of structural maintenance of chromosomes (SMC) proteins. However, none of the proteins encoded by this insertion bears any similarity with a hAT family transposase making the mechanism and the origin of this insertion all the more puzzling.

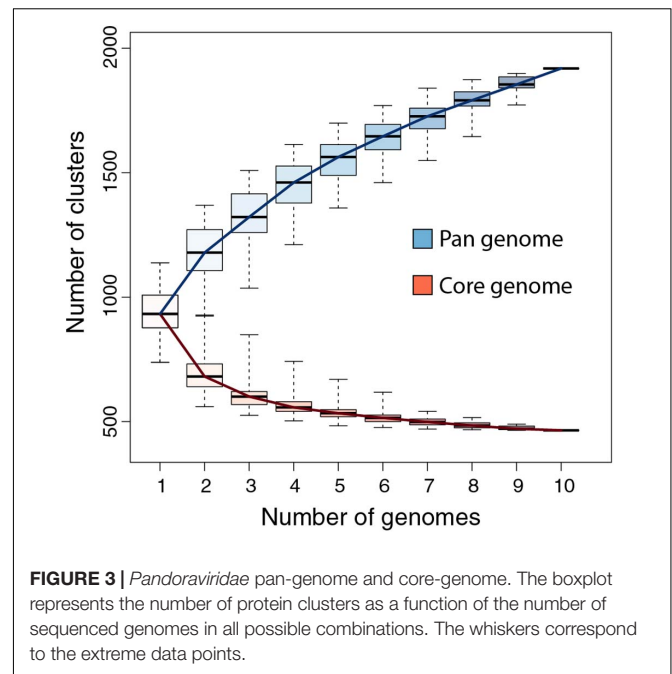
Finally, the proposed scenario concerning  $S_0$  and  $S_2$  are simpler. As the two corresponding transposases (pclt\_cds\_98 and pclt\_cds\_871) are only 91% identical to each other and less than 67% identical to pclt\_cds\_672, we propose that they resulted from two independent insertion events that occurred after the



*p. quercus*/*p. celtis* divergence, from distinct templates with little overlap in their gene cargo (pclt\_cds\_92 and 869) besides active transposases. An alternative scenario, would assume the presence of S<sub>0</sub> and S<sub>2</sub> in the *p. quercus*/*p. celtis* ancestor, and their subsequent excision in *p. quercus*. This scenario is less likely as *p. inopinatum* (Figure 1, node 8) does not encode any hAT transposase.

## Tandem Duplications

Approximately 28 kb downstream from the S<sub>2</sub> transposon (absent in *p. quercus*), the *p. celtis* vs. *p. quercus* dot plot indicates a cluster of closely interspersed direct repeats (Supplementary Figure S3) coding for paralogous proteins that all contain a highly conserved N-terminal fascin-like domain (CD00257). This 80-residue long domain is found in actin-bundling/crosslinking proteins. Many copies of these proteins are found in each of the known pandoraviruses. There are 17 (full-length) copies in *p. quercus*, and 14 in *p. celtis*, the paralogs sharing from 100 to 40% identical residues. Using standard phylogenetic analysis each of the *p. celtis* paralogs are unambiguously clustered with *p. quercus* counterparts in 14 orthologous pairs, indicating that the multiplication of these proteins took place prior to their divergence (Supplementary Figure S3). As the three additional *p. quercus* paralogs (pqr\_cds\_130, 131, and 870) with no obvious counterpart in *p. celtis* are not very similar to other *p. quercus* paralogs (max is 72% sequence identity between pqr\_cds\_870 and pqr\_cds\_869), it is unlikely that they arise from post-divergence duplications. The most parsimonious scenario is thus that their counterparts have been recently lost by *p. celtis*. In a dot plot, the pqr\_cds\_130 and pqr\_cds\_131 genes correspond to a 4 kb deletion at position 224,350 in *p. celtis*. The remaining pqr\_cds\_870 is located in a dense cluster of 6 contiguous



paralogs (pqr\_cds\_866-871) in *p. quercus*, clearly homologous to a similar cluster of 5 contiguous paralogs (pclt\_cds\_884-888) in *p. celtis* (Supplementary Figure S3). The deletion of a short segment of the *p. celtis* genome is visible at this exact position (1,487,300). Another member of this cluster (pclt\_cds\_886) just entered a pseudogenization process through the several insertion/deletions breaking its original reading frame (Supplementary Figure S3).

## Core Genes and Pan Genome Update

We previously designed a stringent gene annotation scheme to minimize overpredictions in G+C-rich genomes. In particular, genes predicted to encode proteins without database homolog (i.e., ORFans) were required to overlap with detected sense transcripts to be validated (Legendre et al., 2018). According to this protocol, *p. celtis* encodes at least 1184 protein-coding genes (CDS) compared to 1185 protein-coding genes for *p. quercus*. Both encode a single tRNA(Pro). It is worth noticing that despite a strong reduction compared to the number of proteins initially predicted by standard methods (Philippe et al., 2013), the proportion of ORFans (i.e., w/o homolog outside of the *Pandoraviridae* family) remains high at 68%. This confirms that the lack of database homologs is not caused by bioinformatics overpredictions (Legendre et al., 2018). *P. celtis* and *p. quercus* shared an average of 96% identical residues, as computed from 822 unambiguous orthologous proteins encoded by single copy genes (i.e., w/o paralogs).

We previously showed that the comparison of the first six available pandoravirus genomes rapidly converged toward a relatively small set of common genes, corresponding to 455 distinct proteins (i.e., clusters) (Legendre et al., 2018). An even smaller estimate (352) was subsequently proposed by another laboratory using a different clustering protocol and

strains (Aherfi et al., 2018). Now based on the ten fully sequenced pandoraviruses and an optimized clustering protocol (see Materials and Methods), the *Pandoraviridae* core gene set was found to contain 464 genes, close to the asymptotic limit suggested by **Figure 3**. Including *p. celtis* in the analysis caused the removal of two proteins from the list. Their homologs in *p. quercus* are *pqr\_cds\_672*, and *pqr\_cds\_370*, two proteins w/o recognizable functional attribute or homolog outside of the *Pandoraviridae*. Compared to the average number of distinct proteins encoded by individual pandoravirus genomes, the proportion of those presumably essential is thus less than half. On the other hand, the predicted gene content of *p. celtis* further increased the *Pandoraviridae* pan-genome. Despite its overall close similarity with *p. quercus*, *p. celtis* remains on a growth curve whereby each new randomly isolated pandoravirus is predicted to add about 60 distinct proteins to the total number of protein clusters already identified in the family (**Figure 3**). The process by which such addition could arise was further investigated by a detailed comparison of the genomes of the most similar relatives, *p. quercus* and *p. celtis*.

### Protein-Coding Genes Unique to *P. celtis* or *P. quercus*

Given the strong similarity between the two genomes, determining their difference in gene content is straightforward. However, these differences can be due to various mechanisms: the duplication of existing genes, their differential loss, their acquisition by horizontal transfer, or their *de novo* creation. Here we wanted to focus on the later mechanism, previously proposed to be prominent in the *Pandoraviridae* family (Legendre et al., 2018). The candidate genes most likely resulting from *de novo* creation would be those unique to *p. celtis* or *p. quercus*. If there are no homolog in any of the other pandoraviruses, *de novo* creation (or acquisition from an unknown source) becomes the most parsimonious evolutionary scenario, compared to a scenario whereby such a gene, present in an ancestral pandoravirus would have been independently lost multiple times. The 30 protein-coding genes unique to *p. celtis* ( $N = 9$ ) and *p. quercus* ( $N = 21$ ) are listed in **Table 1**. As previously noticed (Legendre et al., 2018), these presumed novel genes are associated with statistics that are significantly different from other pandoravirus protein-coding genes. They exhibit a lower Codon Adaptation Index (CAI = 0.233 vs. 0.351, Wilcoxon test,  $p < 10^{-14}$ ), a lower G+C content (57.5% vs. 64.4%,  $p < 10^{-16}$ ), and encode smaller proteins [length (aa) = 126.6 vs. 387.3,  $p < 10^{-15}$ ]. The two later characteristics make them similar to the random ORFs found in intergenic regions (i.e., the so-called “protogenes”) from which we proposed they originated.

We also noticed that the proteins encoded by the novel genes exhibit an amino-acid composition widely different from the rest of the predicted proteome (Chi-2,  $df = 19$ ,  $p < 10^{-10}$ ), with the largest variations observed for lysine (increasing from 2 to 5%), phenylalanine (2.2 to 4%), and arginine (8.6 to 11.3%). Owing to the anomalous proportions of these residues, 25 out of the 30 novel *p. celtis* and *p. quercus* unique proteins are predicted to be DNA-binding (Szilágyi and Skolnick, 2006)

(**Table 1**). Although such predictions are subject to caution (as the predictions remains the same for shuffled sequences) binding novel proteins to the viral genome might help segregate loosely folded (i.e., intrinsically disordered) proteins and diminish their potential interference with the rest of the viral proteome. Over time, these proteins may also gain some regulatory functions.

We investigated the putative intergenic origin of these 30 strain-specific protein-coding genes by searching for remote sequence similarity in the genome of all other pandoraviruses, using tblastn (protein query against six reading frame translation,  $E < 10^{-3}$ ) (Sayers et al., 2019). For seven of them, one unique to *p. celtis* and six unique to *p. quercus*, we found no similarity within the non-coding moiety of other pandoraviruses. Our most parsimonious interpretation is that they represent recent independent additions in each genome by *de novo* creation or transfer from an unknown organism w/o known relative. A slightly less parsimonious scenario would be their addition prior to node 9, followed by differential losses in *p. quercus* or *p. celtis*. Remote but significant ( $E < 10^{-3}$ ) similarities were detected for the 25 other novel genes within non-coding regions of other pandoraviruses, all of them members of Clade A (**Figure 1**). These positive matches were distributed as followed: five in strains that diverged since node 9, eight in all strains that diverged since node 8, four in all strains that diverged since node 5, and six in all strains that diverged since node 2. We did not detect significant matches in earlier diverging Clade B members. The distribution of these traces in pandoraviruses at various evolutionary distances is interpreted in the Section “Discussion.”

### ncRNAs

We annotated 161 ncRNAs in *p. celtis* (**Supplementary Table S1**), a number close to the 157 ncRNAs predicted for *p. quercus* using the same protocol. Such numerous transcripts without protein coding capability were previously noticed for other pandoravirus strains (Legendre et al., 2018). The *p. celtis* ncRNAs vary in length from 234 to 4,456 nucleotides (median = 1384, mean =  $1413 \pm 639$ ). By comparison, the *p. quercus* ncRNAs range from 273 to 5,176 (median = 1,189, mean =  $1299 \pm 738$ ). The two distributions are not significantly different ( $T$ -test:  $p > 0.13$ ). The expression levels (in median read coverage) of *p. celtis* ncRNAs vary from 92 to 1608 (median = 283) compared to 3665–506,994 (median = 690) for protein coding transcripts. A similar non-coding *versus* coding expression median ratio ( $\approx 0.41$ ) was previously found for *p. quercus* (ncRNAs median = 228, protein-coding transcript median = 551), in a distinct experiment. As previously noticed for other pandoravirus strains, most of *p. celtis* ncRNAs (154/161 = 95.6%) are overlapping by more than half of their length with a protein-coding transcript expressed from the opposite strand, and only 7 are mostly intergenic.

Although the *p. celtis* and *p. quercus* genomes share a very large proportion of their protein-coding genes (1146/1184 = 96.8%), this was not the case for ncRNAs. We found that only 87 of *p. celtis* ncRNAs (87/161 = 54%) exhibit a homolog among *p. quercus* ncRNAs (**Supplementary Table S1**). The 74 *p. celtis* ncRNAs without homologs thus mostly correspond to the lack of detectable transcription in the cognate

sequence of the *p. quercus* genome. Unexpectedly, the *p. celtis* and *p. quercus* novel protein-coding genes discussed above (see Protein-Coding Genes Unique to *p. celtis* or *p. quercus*) only rarely overlap with ncRNAs in other strains. The single case is *pclt\_cds\_308*, the coding region of which overlaps with a *p. quercus* ncRNA (*pqer\_ncRNA\_47*) (Table 1).

## Selection Pressure on New Genes

Protein-coding genes shared by at least two different pandoraviruses provide an opportunity to estimate the selection pressure acting on them by computing the ratio of nonsynonymous (dN) to synonymous (dS) substitutions per site. We computed the dN/dS ratio of genes shared by increasingly close pandoraviruses, dating their creation or acquisition by reference to the corresponding node in the pandoravirus phylogenetic tree (nodes 1–9 in Figure 1). All pairs of orthologous gene sequences were thus analyzed using the YN00 algorithm from the PAM package (Yang, 2007) and assigned to their most likely creation/acquisition node based on their presence or absence in various clades of pandoraviruses. As shown in Figure 4 all genes are on average under negative selection pressure (dN/dS < 1), including the presumably most recently created/acquired genes as those only found in *p. quercus* and *p. celtis* (i.e., node 9 in Figure 1). As previously documented for short evolutionary distances and very close gene sequences (our case), the computed dN/dS values are probably overestimated (i.e., closer to 1) given that a fraction of the deleterious mutations might not yet be fixed (Rocha et al., 2006). This is consistent with the observed negative correlation between the depth of creation/acquisition and the computed purifying selection (Figure 4). In other words recently created/acquired genes appear under selective constraints weaker than that of “older” genes. The fact that dN/dS values tend to decrease with longer divergence times was previously noticed (Rocha et al., 2006).

## DISCUSSION

Following our previous analysis of 6 available members of the *Pandoraviridae* family, we proposed that the gigantism of their genomes as well as the large proportion of ORFans among their encoded proteins was the result of unusual evolutionary mechanisms, including *de novo* gene creation from previously non-coding sequences (Legendre et al., 2018). In this previous study, we compared pandoravirus isolates exhibiting pairwise similarity ranging from 54 to 88%, as computed from a super alignment of their orthologous proteins. At such evolutionary distances, the observed differences are most often the result of multiple and overlapping elementary variation processes the succession of which becomes impossible to retrace. The subsequent isolation of *p. celtis*, a new pandoravirus strain very similar to *p. quercus* (with orthologous proteins sharing 96% of identical residues in average), gave us the opportunity of identifying and estimating the relative contributions of various types of genomic alterations at work during their microevolution from their recent common ancestor.

The global analyses of the gene contents of the 10 members of the *Pandoraviridae* family available today confirmed previous estimates of the number of core gene clusters (Aherfi et al., 2018; Legendre et al., 2018) at 464. Such a small proportion (less than half) of presumably “essential” genes compared to the total number of proteins encoded by each pandoravirus genome (ranging from 1070 to 1430, using our stringent protocol) (Legendre et al., 2018) raises the question of the origin and utility of so many “accessory” genes. Non-essential genes are normally eliminated from the genomes of obligate intracellular parasites or symbionts through reductive evolution (Corradi et al., 2010; Lopez-Madrugal et al., 2011; McCutcheon and Moran, 2011; Latorre and Manzano-Marín, 2017; Floriano et al., 2018). The contrast is even more puzzling when the size of the *Pandoraviridae* pan-genome shows no sign of leveling off after reaching 1910 different protein-coding gene clusters, sustaining a trend predicting that each new isolate will contribute 60 additional clusters. Understanding the mechanism by which new genes, - most of which encode ORFans -, appear in the genome of pandoraviruses was the main goal of our study.

As we investigated the most visible alterations of the otherwise nearly perfect collinearity of the *p. celtis* and *p. quercus* genomes, we identified 3 transposons of the hAT family (*S*<sub>0</sub>, *S*<sub>1</sub>, and *S*<sub>2</sub> in Figure 2). The cargo of these mobile elements was found to be variable in gene number (10 for *S*<sub>0</sub>, 11 for *S*<sub>1</sub>, and 7 for *S*<sub>2</sub>) and with a single overlap (*pclt\_cds\_92*, 681, 869) in addition to the transposases. These by-standing proteins exhibit no functional signature and have no homolog outside of the *Pandoraviridae* family. Interestingly, hAT family transposases have recently been identified in various *Acanthamoeba* species (Zhang et al., 2018). However, the gene contents of the *p. celtis* and *p. quercus* hAT transposons indicates that these mobile elements are not prominent vehicles of lateral gene transfers from the amoebal hosts to the pandoraviruses. With the exception of *pclt\_cds\_870* (encoded by *S*<sub>2</sub>), newly inserted transposons do not contribute genes unique to *p. celtis*. The hAT transposable elements only appear to ferry genes between pandoravirus strains, generating non-local duplications. Such exchanges might occur within an amoebal host undergoing multiple infections. To our knowledge, this is the first identification of hAT family transposons in DNA viruses. The fact that hAT transposons are not present in other well-documented families of large and giant virus infecting *Acanthamoeba* (Abergel et al., 2015; Aherfi et al., 2016; Fabre et al., 2017; Zhang et al., 2018) suggests that its transfer from host to virus is a rare event, or is specifically linked to pandoravirus infections.

This work identified 30 genes unique to *p. celtis* or *p. quercus* (Table 1) that we interpreted as encoding novel proteins that appeared after the recent divergence of these two strains from their common ancestor (i.e., below node 9 in Figure 1). These new genes are uniformly distributed along the *p. celtis* and *p. quercus* genomes, and do not colocalize with large genomic insertions or rearrangements, except for *pqer\_cds\_665* and *pqer\_cds\_673* encoded by the 30.5 kb segments unique to *p. quercus* (see Main Structural Features of the *p. celtis* and *p. quercus* Genomes). As noticed in our previous study (Legendre et al., 2018) all these proteins

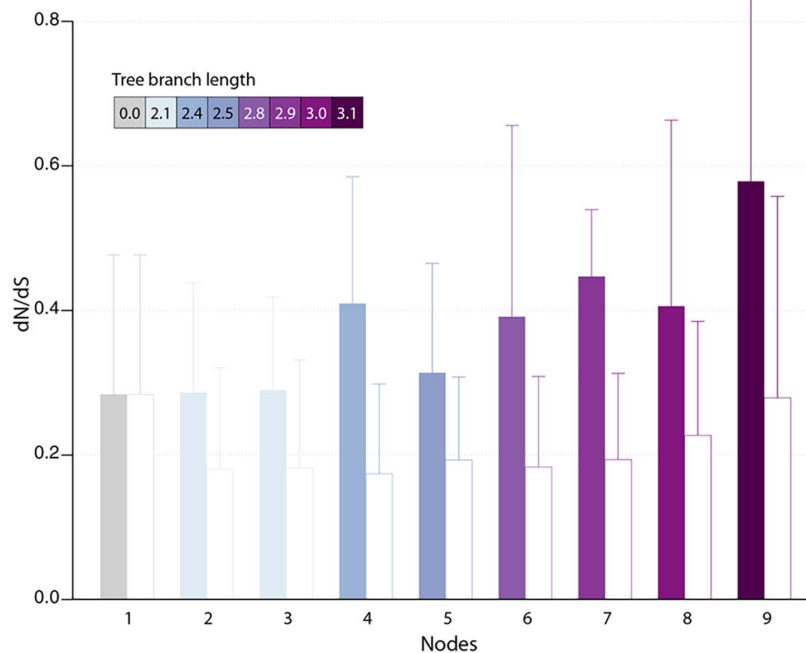


**FIGURE 4** | Estimated selection pressure acting on pandoravirus genes as a function of their ancestry. Shown is the mean of dN/dS ratios (filled bars) for genes that are unique to the pandoravirus strains below a given node in their phylogeny tree (see **Figure 1**). Error bars correspond to standard deviations. Bars are colored according to the depth of the node in the tree. As a control, we calculated the dN/dS of pandoraviruses' core genes (empty bars). For a given node, we considered pairs of orthologous genes whose common ancestor correspond to that node.

are strict ORFans (not detected in any other organism, virus or other pandoravirus strains) and exhibit statistical features different from other pandoravirus genes, including a G+C content closer to that of non-coding/intergenic regions. We thus proposed that new proteins could be *de novo* created by the triggering of the transcription and translation of pre-existing non-coding sequences (the so-called “protogenes”). Here we further investigated this hypothesis by looking for eventual similarities of the new protein sequences with non-coding regions in other pandoraviruses at increasing evolutionary distances (**Figure 1**). For 8 of the 9 new *p. celtis* proteins and 15 of the 21 new *p. quercus* proteins we detected significant non-coding matches in various pandoravirus strains, in good agreement with their phylogenetic relationships. Trace of five new genes were only detected at the level of node 9, 8 at the more ancient node 8, 4 at the node 5, and 6 at the root (node 2) of the clade A pandoraviruses. Although these numbers are small and subject to fluctuations, such a distribution of hits suggests an evolutionary process combining a continuous spontaneous generation of open reading frames, followed by their drift back as non-coding sequences, unless they become transcriptionally active, and fixed as new proteins in a given strain. The maximum value of detected traces at node 8 might thus result from a compromise between the time interval required to generate *de novo* proteins, and the time during which they could retain a detectable similarity with the drifting non-coding regions from which they originated.

According to the above gene creation hypothesis, initially non-coding regions could act as precursors for new proteins, by the random opening of a suitable reading frame, followed by its transcriptional activation. Such a scenario is compatible with the distribution of new gene matches in other pandoravirus strains discussed above, where 8 correspond to intergenic regions, and 5 overlap with UTRs (**Table 1**). The flexibility of intergenic regions is further attested by the fact that 11 of the new genes have no matches. As shown in **Table 1**, a single new gene (*pclt\_cds\_308*) was found to co-localize with a ncRNA (*pqer\_ncRNA\_47*) despite the large number of ncRNAs detected in the *p. celtis* and *p. quercus* genomes. ncRNAs thus do not appear to be necessary intermediates in the emergence of new proteins. The low proportion of conserved ncRNAs between the two close strains (54%) suggests that the on/off expression status of non-coding genomic sequences is fluctuating very fast, and may even be variable at the viral population level.

The fact that a negative selection pressure ( $dN/dS < 1$ ) is associated to the genes appeared since the divergence of *p. celtis* and *p. quercus* decisively reinforces the hypothesis of their *de novo* creation. Firstly, it provides the proof that these genes are truly expressed as *bona fide* proteins, given that differences between synonymous vs. non-synonymous mutations cannot be generated within non-translated nucleotide sequences. Any significant deviation from neutrality ( $dN/dS \approx 1$ ) can only be due to a selection process exerted on certain amino acids at certain



positions of a true protein in order to improve, preserve, or eliminate its function.

The analysis of proteins whose creation appears most recent (node 9 in **Figure 4**) indicates a negative selection pressure whose (probably overestimated) average value (0.58) could correspond to functions slightly increasing the pandoravirus fitness. However, the interpretation of the selection pressure in the context of a function is a problem here, since we previously pointed out that it is highly unlikely that a newly created small protein will have a function (enzymatic, regulatory or structural) in the first place, even less a beneficial one (Legendre et al., 2018).

Thus, we propose an alternative interpretation, based on the knowledge accumulated over the years on the principles governing the stability of proteins. According to our scenario, most new proteins are from the translation of pre-existing non-coding "protogenes" (see Protein-Coding Genes Unique to *p. celtis* or *p. quercus*) and the rest from DNA inserts of unknown origin (such as pqr\_cds\_665 and pqr\_cds\_673). It is then unlikely that many of these new proteins lacking an evolutionary history will adopt a globular fold (Monsellier and Chiti, 2007; Watters et al., 2007; Tanaka et al., 2010). Most will be toxic by causing nonspecific aggregations within the host-virus proteome and be quickly eliminated through the reversal of these newborn viral genes to an untranscribed/untranslated state. In contrast, proteins whose folded 3-D structures do not prove to be toxic will enter an evolutionary process involving a negative selection pressure promoting the conservation of the amino acids responsible for their stability. Their proportion was estimated at about 34% for 100–200 residue proteins (Miao et al., 2004). In absence of an initial function, the other positions/residues will evolve in a neutral manner. Once "fixed," the new genes will exhibit an average selection pressure lower than one, combining 1/3 of negative selection with 2/3 of neutrality. Following many studies that have concluded that efficient folding (Watters et al., 2007) and prevention of aggregation are important drivers of protein evolution (see Monsellier and Chiti, 2007), our scenario predicts that many genes specific to pandoraviruses should encode proteins not increasing their fitness, but whose stable 3-D structures may eventually serve as innovative platforms for new functions.

## CONCLUSION

The detailed comparative analysis of *p. celtis* with its very close relative *p. quercus* enabled us to estimate the contributions of various microevolutionary processes to the steady increase of the pan-genome of the *Pandoraviridae* giant virus family. We first showed that large-scale genomic rearrangements (segmental duplications, translocations) are associated to transposable elements of the hAT family, widespread in metazoans, but until now unique to this family of viruses. However, these mobile elements mostly appear to shuffle pandoravirus genes between strains, without creating new ones or promoting host-to-virus horizontal gene transfers. In contrast with the popular view that horizontal gene transfer plays an important role in the evolution of large DNA viruses (Yutin and Koonin, 2013;

Koonin et al., 2015; Schulz et al., 2017), this is definitely not a main cause of genome inflation in the *Pandoraviridae*, as we previously argued (Claverie and Abergel, 2013; Philippe et al., 2013; Abergel et al., 2015; Legendre et al., 2018). Finally, we also found that locally repeated regions are the siege of a competition between tandem duplication and gene deletion, locally reshaping the genomes without contributing to net genetic innovation (**Supplementary Figure S3**).

In continuity with our previous work on more distant pandoravirus strains, we found that the 30 protein-coding genes born since the divergence between the very close *p. quercus* and *p. celtis* strains were derived from preexisting non-coding sequences or small DNA segments of unknown origins inserted at randomly interspersed locations. We propose that random ORFs constantly emerge in non-coding regions and that their transcription is turned on in some pandoravirus strains, while they remain silent until they are deleted or diverge beyond recognition in others strains. Our results add strong support to the constant *de novo* creation of proteins, few of which are retained with a little initial impact on the virus fitness until eventually acquiring a selectable function.

Such a scenario, particularly visible and active in the *Pandoraviridae*, might also apply to the large proportion of ORFans encoded by other DNA viruses, from large eukaryotic viruses (Abergel et al., 2015) to much smaller bacteriophages, in which they can be the target of global functional studies (Berjón-Otero et al., 2017). Interestingly, the *de novo* gene creation scenario is gaining more and more acceptance beyond the realm of virology, recently to explain the origin of orphan protein even in mammals (Schmitz et al., 2018).

## DATA AVAILABILITY

*P. celtis*' annotated genome is deposited in GenBank under Accession n° MK174290.

## AUTHOR CONTRIBUTIONS

CA, ML, J-MC, and YC designed the experiments. J-MA, AL, NP, SJ, and YC contributed to the data and performed the experiments. ML, SN, NT, OP, CA, and J-MC analyzed the data. ML, CA, and J-MC wrote the manuscript.

## FUNDING

This work was partially supported by the French National Research Agency (ANR-14-CE14-0023-01), France Genomique (ANR-10-INBS-01-01), Institut Français de Bioinformatique (ANR-11-INBS-0013), the Fondation Bettencourt-Schueller (OTP51251), by a DGA-MRIS scholarship, and by the Provence-Alpes-Côte-d'Azur région (2010 12125). Proteomic experiments were partly supported by the Proteomics French Infrastructure (ANR-10-INBS-08-01) and Labex GRAL (ANR-10-LABX-49-01). We thank the support of the discovery platform and informatics group at EDyP and the PACA-Bioinfo platform.

## ACKNOWLEDGMENTS

We kindly thank Hua-Hao Zhang for providing us with the hAT-transposon sequence he identified in the *Acanthamoeba castellanii* genome.

## REFERENCES

- Abergel, C., Legendre, M., and Claverie, J. M. (2015). The rapidly expanding universe of giant viruses: mimivirus, pandoravirus, pithovirus and mollivirus. *FEMS Microbiol. Rev.* 39, 779–796. doi: 10.1093/femsre/fuv037
- Aherfi, S., Andreani, J., Baptiste, E., Oumessoum, A., Dornas, F. P., Andrade, A. C. D. S. P., et al. (2018). A large open pangenome and a small core genome for giant pandoraviruses. *Front. Microbiol.* 9:1486. doi: 10.3389/fmicb.2018.01486
- Aherfi, S., Colson, P., La Scola, B., and Raoult, D. (2016). Giant viruses of amoebas: an update. *Front. Microbiol.* 7:349. doi: 10.3389/fmicb.2016.00349
- Antwerpen, M. H., Georgi, E., Zoeller, L., Woelfel, R., Stoecker, K., and Scheid, P. (2015). Whole-genome sequencing of a pandoravirus isolated from keratitis-inducing acanthamoeba. *Genome Announc.* 3:e00136–15. doi: 10.1128/genomeA.00136-15
- Atkinson, P. W. (2015). hAT transposable elements. *Microbiol. Spectr.* 3:MDNA3-0054-2014. doi: 10.1128/microbiolspec.MDNA3-0054-2014
- Berjón-Otero, M., Lechuga, A., Mehla, J., Uetz, P., Salas, M., and Redrejo-Rodríguez, M. (2017). Bam35 tectivirus intraviral interaction map unveils new function and localization of phage ORFan proteins. *J. Virol.* 91:e0870–17. doi: 10.1128/JVI.00870-17
- Chin, C. S., Alexander, D. H., Marks, P., Klammer, A. A., Drake, J., Heiner, C., et al. (2013). Nonhybrid, finished microbial genome assemblies from long-read SMRT sequencing data. *Nat. Methods* 10, 563–569. doi: 10.1038/nmeth.2474
- Claverie, J. M., and Abergel, C. (2013). Open questions about giant viruses. *Adv. Virus Res.* 85, 25–56. doi: 10.1016/B978-0-12-408116-1.00002-1
- Claverie, J. M., Abergel, C., and Legendre, M. (2018). Giant viruses that create their own genes. *Med. Sci.* 34, 1087–1091. doi: 10.1051/medsci/2018300
- Corradi, N., Pombert, J. F., Farinelli, L., Didier, E. S., and Keeling, P. J. (2010). The complete sequence of the smallest known nuclear genome from the microsporidian *Encephalitozoon intestinalis*. *Nat. Commun.* 1:77. doi: 10.1038/ncomms1082
- Emms, D. M., and Kelly, S. (2015). OrthoFinder: solving fundamental biases in whole genome comparisons dramatically improves orthogroup inference accuracy. *Genome Biol.* 16:157. doi: 10.1186/s13059-015-0721-2
- Fabre, E., Jeudy, S., Santini, S., Legendre, M., Trauchessec, M., Couté, Y., et al. (2017). Noumeavirus replication relies on a transient remote control of the host nucleus. *Nat. Commun.* 8:15087. doi: 10.1038/ncomms15087
- Floriano, A. M., Castelli, M., Krenek, S., Berendonk, T. U., Bazzocchi, C., Petroni, G., et al. (2018). The genome sequence of "*Candidatus Fokinia solitaria*": insights on reductive evolution in rickettsiales. *Genome Biol. Evol.* 10, 1120–1126. doi: 10.1093/gbe/evy072
- Grabherr, M. G., Haas, B. J., Yassour, M., Levin, J. Z., Thompson, D. A., Amit, I., et al. (2011). Full-length transcriptome assembly from RNA-Seq data without a reference genome. *Nat. Biotechnol.* 29, 644–652. doi: 10.1038/nbt.1883
- Hoang, D. T., Chernomor, O., von Haeseler, A., Minh, B. Q., and Vinh, L. S. (2018). UFBoot2: improving the ultrafast bootstrap approximation. *Mol. Biol. Evol.* 35, 518–522. doi: 10.1093/molbev/msx281
- Katoh, K., Misawa, K., Kuma, K., and Miyata, T. (2002). MAFFT: a novel method for rapid multiple sequence alignment based on fast Fourier transform. *Nucleic Acids Res.* 30, 3059–3066. doi: 10.1093/nar/gkf436
- Koonin, E. V., Krupovic, M., and Yutin, N. (2015). Evolution of double-stranded DNA viruses of eukaryotes: from bacteriophages to transposons to giant viruses. *Ann. N. Y. Acad. Sci.* 1341, 10–24. doi: 10.1111/nyas.12728
- Krumsiek, J., Arnold, R., and Rattei, T. (2007). Gepard: a rapid and sensitive tool for creating dotplots on genome scale. *Bioinformatics* 23, 1026–1028. doi: 10.1093/bioinformatics/btm039
- Kumar, S., Stecher, G., Li, M., Knyaz, C., and Tamura, K. (2018). MEGA X: molecular evolutionary genetics analysis across computing platforms. *Mol. Biol. Evol.* 35, 1547–1549. doi: 10.1093/molbev/msy096
- Latorre, A., and Manzano-Marín, A. (2017). Dissecting genome reduction and trait loss in insect endosymbionts. *Ann. N. Y. Acad. Sci.* 1389, 52–75. doi: 10.1111/nyas.13222
- Legendre, M., Fabre, E., Poirot, O., Jeudy, S., Lartigue, A., Alempic, J. M., et al. (2018). Diversity and evolution of the emerging *Pandoraviridae* family. *Nat. Commun.* 9:2285. doi: 10.1038/s41467-018-04698-4
- Legendre, M., Lartigue, A., Bertaux, L., Jeudy, S., Bartoli, J., Lescot, M., et al. (2015). In-depth study of mollivirus sibericum, a new 30,000-y-old giant virus infecting *Acanthamoeba*. *Proc. Natl. Acad. Sci. U.S.A.* 112, E5327–E5335. doi: 10.1073/pnas.1510795112
- Lopez-Madrigal, S., Latorre, A., Porcar, M., Moya, A., and Gil, R. (2011). Complete genome sequence of '*Candidatus Tremblaya princeps*' strain PCVAL, an intriguing translational machine below the living-cell status. *J. Bacteriol.* 193, 5587–5588. doi: 10.1128/JB.05749-11
- Marchler-Bauer, A., and Bryant, S. H. (2004). CD-Search: protein domain annotations on the fly. *Nucleic Acids Res.* 32, W327–W331. doi: 10.1093/nar/gkh454
- McCutcheon, J. P., and Moran, N. A. (2011). Extreme genome reduction in symbiotic bacteria. *Nat. Rev. Microbiol.* 10, 13–26. doi: 10.1038/nrmicro2670
- Miao, J., Klein-Seetharaman, J., and Meirovitch, H. (2004). The optimal fraction of hydrophobic residues required to ensure protein collapse. *J. Mol. Biol.* 344, 797–811. doi: 10.1016/j.jmb.2004.09.061
- Monsellier, E., and Chiti, F. (2007). Prevention of amyloid-like aggregation as a driving force of protein evolution. *EMBO Rep.* 8, 737–742. doi: 10.1038/sj.embor.7401034
- Philippe, N., Legendre, M., Doutre, G., Couté, Y., Poirot, O., Lescot, M., et al. (2013). Pandoraviruses: amoeba viruses with genomes up to 2.5 Mb reaching that of parasitic eukaryotes. *Science* 341, 281–286. doi: 10.1126/science.1239181
- Remmert, M., Biegert, A., Hauser, A., and Söding, J. (2011). HHblits: lightning-fast iterative protein sequence searching by HMM-HMM alignment. *Nat. Methods* 9, 173–175. doi: 10.1038/nmeth.1818
- Rice, P., Longden, I., and Bleasby, A. (2000). EMBOSS: the European molecular biology open software suite. *Trends Genet.* 16, 276–277. doi: 10.1016/S0168-9525(00)02024-2
- Rocha, E. P. C., Smith, J. M., Hurst, L. D., Holden, M. T., Cooper, J. E., Smith, N. H., et al. (2006). Comparisons of dN/dS are time dependent for closely related bacterial genomes. *J. Theor. Biol.* 239, 226–235. doi: 10.1016/j.jtbi.2005.08.037
- Sayers, E. W., Agarwala, R., Bolton, E. E., Brister, J. R., Canese, K., Clark, K., et al. (2019). Database resources of the national center for biotechnology information. *Nucleic Acids Res.* 47, D23–D28. doi: 10.1093/nar/gky1069
- Schmitz, J. F., Ullrich, K. K., and Bornberg-Bauer, E. (2018). Incipient *de novo* genes can evolve from frozen accidents that escaped rapid transcript turnover. *Nat. Ecol. Evol.* 2, 1626–1632. doi: 10.1038/s41559-018-0639-7
- Schulz, F., Yutin, N., Ivanova, N. N., Ortega, D. R., Lee, T. K., Vierheilig, J., et al. (2017). Giant viruses with an expanded complement of translation system components. *Science* 356, 82–85. doi: 10.1126/science.aal4657
- Szilágyi, A., and Skolnick, J. (2006). Efficient prediction of nucleic acid binding function from low-resolution protein structures. *J. Mol. Biol.* 358, 922–933. doi: 10.1016/j.jmb.2006.02.053
- Tanaka, J., Doi, N., Takashima, H., and Yanagawa, H. (2010). Comparative characterization of random-sequence proteins consisting of 5, 12, and 20 kinds of amino acids. *Protein Sci.* 19, 786–795. doi: 10.1002/pro.358
- Watters, A. L., Deka, P., Corrent, C., Callender, D., Varani, G., Sosnick, T., et al. (2007). The highly cooperative folding of small naturally occurring proteins is

## SUPPLEMENTARY MATERIAL

The Supplementary Material for this article can be found online at: <https://www.frontiersin.org/articles/10.3389/fmicb.2019.00430/full#supplementary-material>

- likely the result of natural selection. *Cell* 128, 613–624. doi: 10.1016/j.cell.2006.12.04
- Yang, Z. (2007). PAML 4: phylogenetic analysis by maximum likelihood. *Mol. Biol. Evol.* 24, 1586–1591. doi: 10.1093/molbev/msm088
- Yutin, N., and Koonin, E. V. (2013). pandoraviruses are highly derived phycodnaviruses. *Biol. Direct.* 8:25. doi: 10.1186/1745-6150-8-25
- Zhang, H. H., Zhou, Q. Z., Wang, P. L., Xiong, X. M., Luchetti, A., Raoult, D., et al. (2018). Unexpected invasion of miniature inverted-repeat transposable elements in viral genomes. *Mob. DNA* 9:19. doi: 10.1186/s13100-018-0125-4

**Conflict of Interest Statement:** The authors declare that the research was conducted in the absence of any commercial or financial relationships that could be construed as a potential conflict of interest.

Copyright © 2019 Legendre, Alempic, Philippe, Lartigue, Jeudy, Poirot, Ta, Nin, Couté, Abergel and Claverie. This is an open-access article distributed under the terms of the Creative Commons Attribution License (CC BY). The use, distribution or reproduction in other forums is permitted, provided the original author(s) and the copyright owner(s) are credited and that the original publication in this journal is cited, in accordance with accepted academic practice. No use, distribution or reproduction is permitted which does not comply with these terms.